Thermoelectric Properties of $Re_3Ge_{0.6}As_{6.4}$ and Re_3GeAs_6 in Comparison to $Mo_3Sb_{5.4}Te_{1.6}$

Navid Soheilnia,[†] Hong Xu,[†] Huqin Zhang,[‡] Terry M. Tritt,[‡] Ian Swainson,[§] and Holger Kleinke*[,§]

Department of Chemistry, University of Waterloo, Waterloo, Ontario, Canada N2L 3G1, Department of Physics and Astronomy, Clemson University, Clemson, South Carolina 29634-0978, and Chalk River Laboratories, Chalk River, Ontario, Canada K0J 1J0

Received March 27, 2007. Revised Manuscript Received June 5, 2007

Heavily doped narrow gap semiconductors with complex crystal structures are prime candidates for thermoelectric materials. The arsenides $Re_3(Ge,As)_7$ are new examples with promising thermoelectric properties, comparable with the isostructural $Mo_3Sb_{5.4}Te_{1.6}$, a competitive high-temperature material. Various doping levels may be achieved by using different Ge/As ratios. $Re_3(Ge,As)_7$ was prepared by heating the elements in the desired ratios in evacuated silica tubes between 600 and 800 °C. Re_3GeAs_6 crystallizes in the cubic Ir_3Ge_7 type, space group $Im\bar{3}m$, with $a = 8.73202(8)$ Å. It exhibits high Seebeck coefficient, high electrical conductivity, and reasonably low thermal conductivity. Moreover, the thermoelectric figure-of-merit $ZT = TS^2\sigma/\kappa$ increases rapidly with increasing temperature, as desired for high-temperature thermoelectrics.

Introduction

Thermoelectric materials are commercially used for both power generation utilizing the Seebeck effect and cooling applications utilizing the Peltier effect. Waste heat, e.g., that stemming from combustion in car engines, may be used for the former effect. With natural resources declining, this fascinating energy conversion enjoys increasing attention. Experience shows that the best materials are narrow band gap semiconductors composed of heavy elements, exhibiting large Seebeck coefficient, S, combined with high electrical conductivity, σ, and low thermal conductivity, κ.[1−4] Thermoelectric materials may be classified by comparing the figure-of-merit, ZT, defined as

$$ZT = TS^2\sigma/\kappa \quad (1)$$

New materials with ZT values higher than the commercial materials continue to be found, e.g., the filled skutterudites,[5] $CsBi_4Te_6$[6], $Yb_{14}MnSb_{11}$,[7] and $AgPb_mSbTe_{2+m}$.[8] In 2002, we added to the semiconductors of interest a new material, $Mo_3Sb_{5+\delta}Te_{2-\delta}$,[9] which is a ternary variant of the metallic antimonide Mo_3Sb_7 (Ir_3Ge_7 type).[10,11] Subsequently, $Mo_3Sb_{5.4}Te_{1.6}$ was characterized as one of the leading high-temperature *p*-type thermoelectrics, reaching $ZT = 0.8$ at 1050 K, a value that is comparable to the best filled skutterudites, and even outperforming them in a small temperature range.[12] Adding cations such as nickel into its cubic void leads to a slight albeit significant improvement in its thermoelectric properties.[13] The isostructural $Nb_3Sb_2Te_5$, on the other hand, does not exhibit good thermoelectric properties, with its ZT value at 300 K being 75 times smaller than the one of $Mo_3Sb_{5.4}Te_{1.6}$.[14]

In contrast to the large skutterudite family, where many variants are under investigation, thus far only one material of the Ir_3Ge_7 type is known to have advanced thermoelectric properties, namely $Mo_3Sb_{5+\delta}Te_{2-\delta}$. Most representatives of this type are germanides or stannides without a band gap in the band structure.[11] As well, Re_3As_7[15] with its v.e. = 56 is metallic,[16] like Mo_3Sb_7 with v.e. = 53. Our calculations utilizing the LMTO method[17,18] showed that the hitherto unknown ternary Re_3GeAs_6 (v.e. = 55) should be semicon-

* To whom correspondence should be addressed. E-mail: kleinke@uwaterloo.ca.
† University of Waterloo.
‡ Clemson University.
§ Chalk River Laboratories.

(1) Ioffe, A. F. *Physics of Semiconductors*; Academic Press: New York, 1960.
(2) Rowe, D. M. *CRC Handbook of Thermoelectrics*; CRC Press: Boca Raton, FL, 1995.
(3) Tritt, T. M. *Science* **1999**, *283*, 804−805.
(4) DiSalvo, F. J. *Science* **1999**, *285*, 703−706.
(5) Sales, B. C.; Mandrus, D.; Williams, R. K. *Science* **1996**, *272*, 1325−1328.
(6) Chung, D.-Y.; Hogan, T.; Brazis, P.; Rocci-Lane, M.; Kannewurf, C.; Bastea, M.; Uher, C.; Kanatzidis, M. G. *Science* **2000**, *287*, 1024−1027.
(7) Brown, S. R.; Kauzlarich, S. M.; Gascoin, F.; Snyder, G. J. *Chem. Mater.* **2006**, *18*, 1873−1877.
(8) Hsu, K. F.; Loo, S.; Guo, F.; Chen, W.; Dyck, J. S.; Uher, C.; Hogan, T.; Polychroniadis, E. K.; Kanatzidis, M. G. *Science* **2004**, *303*, 818−821.
(9) Dashjav, E.; Szczepenowska, A.; Kleinke, H. *J. Mater. Chem.* **2002**, *12*, 345−349.
(10) Brown, A. *Nature* **1965**, *206*, 502−503.
(11) Häussermann, U.; Elding-Pontén, M.; Svensson, C.; Lidin, S. *Chem.−Eur. J.* **1998**, *4*, 1007−1015.
(12) Gascoin, F.; Rasmussen, J.; Snyder, G. J. *J. Alloys Compd.* **2007**, *427*, 324−329.
(13) Zhang, H.; He, J.; Zhang, B.; Su, Z.; Tritt, T. M.; Soheilnia, N.; Kleinke, H. *J. Electron. Mater.* **2007**, in press.
(14) Soheilnia, N.; Giraldi, J.; Assoud, A.; Zhang, H.; Tritt, T. M.; Kleinke, H. *J. Alloys Compd.* **2006**, in press.
(15) Furuseth, S.; Kjekshus, A. *Acta Chem. Scand.* **1966**, *20*, 245−250.
(16) Jensen, P.; Kjekshus, A.; Skansen, T. *J. Less-Common Met.* **1969**, *17*, 455−458.
(17) Andersen, O. K. *Phys. Rev. B* **1975**, *12*, 3060−3083.
(18) Skriver, H. L. *The LMTO Method*; Springer: Berlin, Germany, 1984.

10.1021/cm0708517 CCC: $37.00
Published on Web 07/11/2007

ducting like $Mo_3Sb_5Te_2$ (v.e. = 55). With this contribution, we present the physical properties of the promising $Re_3(Ge,As)_7$ series.

Experimental Section

Synthesis and Analysis. The elements used, rhenium (powder, −325 mesh, 99.99), germanium (powder, −100 mesh, 99.999%), arsenic (lump, 99.999%), were acquired from Alfa Aesar and then stored in an argon glove box. The compounds were synthesized by heating the elements in the desired ratios in evacuated silica tubes at temperatures between 600 and 800 °C. To achieve faster homogenization, we shook the tubes after a few days, and then reheated them for a total of 14 days. Phase pure samples of $Re_3Ge_\delta As_{7-\delta}$ could be prepared with $\delta = 1.0$, 0.8, 0.6, and 0.4, whereas side products were found when $\delta = 1.2$, as analyzed by means of X-ray powder diffraction using an INEL powder diffractometer with a position-sensitive detector. All these powder diagrams exhibited only the reflections calculated for Re_3As_7, albeit shifted toward smaller angles (hinting toward a larger unit cell), confirming the structure type as well as the incorporation of Ge into this structure, as no side products were found.

The four samples of the nominal compositions Re_3GeAs_6, $Re_3Ge_{0.8}As_{6.2}$, $Re_3Ge_{0.6}As_{6.4}$ and $Re_3Ge_{0.4}As_{6.6}$ were analyzed by means of standardless energy-dispersive spectroscopy (EDS, LEO 1530, with integrated EDAX Pegasus 1200) using an acceleration voltage of 21 kV. The distribution of Re, Ge, and As appeared to be homogeneous throughout each sample; no additional peaks, and hence no heteroelements, were detected.

Structure Determination. Although X-ray diffraction cannot be used to distinguish between Ge and As or between Sb and Te, the neutron scattering factors of the main group elements are significantly different in Re_3GeAs_6, which is not the case for $Mo_3Sb_5Te_2$ (Ge, +8.19 fm; As, +6.58 fm; Sb, +5.57 fm; Te, +5.68 fm). Therefore, we performed neutron diffraction experiments on the sample Re_3GeAs_6 to verify the expected preference of Ge for the 16f site, i.e., the position with the short homonuclear bond. The corresponding preference of Te for the Sb1 site of Mo_3Sb_7 was postulated on the basis of electronegativity considerations, but not investigated, because neither X-ray nor neutron diffraction experiments could differentiate between Sb and Te.[9]

The neutron diffraction data were collected on the C2 constant wavelength (1.3302 Å) diffractometer at Chalk River Laboratories at room temperature over a period of 12 h.[19] For the Rietveld refinements on Re_3GeAs_6 using GSAS,[20] we compared two models, one with all Ge on the 12d site (i.e., 33.3% Ge and 66.7% As) and one with all Ge on the 16f site (25% Ge and 75% As). The latter model (refinement shown in the supplement) yielded better residual factors, e.g., $R_P = 3.58$ vs 3.78%, and unambiguous displacement parameters ($U_{12d}/U_{16f} = 0.74$) in contrast to the former model ($U_{12d}/U_{16f} = 3.33$). Attempts to refine the occupancies failed. No evidence for Ge/As ordering on the 16f site was found, e.g., a symmetry reduction to $R\bar{3}m$ gives rise to two independent sites (multiplicities 2 and 6 in the primitive setting) of the 16f position of the $Im\bar{3}m$ model, but the refinements yielded statistical distributions of Ge on these two sites in $R\bar{3}m$. As well, no supercell reflections were observed. Crystallographic details of the best refinement with Ge on the 16f site (E2) are shown in Table 1, and atomic positions and displacement parameters in Table 2. To confirm the purity of the $Re_3Ge_{0.6}As_{6.4}$, we carried out Rietveld refinements using X-ray data obtained at room temperature over a period of 15 h (INEL, Cu $K_{\alpha 1}$ radiation). The refinement, shown in the supplement, yielded comparable results, and a slightly smaller cell ($a = 8.7287(3)$ Å).

Table 1. Crystallographic Data from the Neutron Diffraction Experiment on Re_3GeAs_6

empirical formula	Re_3GeAs_6
fw (g mol^{-1})	1080.75
T (K)	298
wavelength (Å)	1.3302
space group	$Im\bar{3}m$
cell dimensions, a (Å)	8.73180(7)
V (Å^3)	665.75(2)
no. of formula units per cell	4
calcd density (g cm^{-3})	10.78
2θ range (deg)	4.9−115.1
R_{F^2}, R_P, R_{wP}	0.0265, 0.0358, 0.0482

Table 2. Atomic Positions and Displacement Parameters of Re_3GeAs_6

atom	site	x	y	z	U_{eq} (Å^2)	occupancy
Re	12e	0.3413(2)	0	0	0.0017(3)	1 Re
As1	12d	1/4	0	1/2	0.0054(5)	1 As
E2	16f	0.1663(2)	0.1663(2)	0.1663(2)	0.0073(4)	0.25 Ge, 0.75 As

Electronic Structure Calculations. The LMTO method (LMTO = linear muffin tin orbitals) was utilized with the atomic spheres approximation (ASA)[17,18] for the electronic structure calculations. In the LMTO approach, the density functional theory is used with the local density approximation (LDA) to treat correlation effects.[21] The following wavefunctions were used: for Re, 6s, 6p, 5d and 5f (5f downfolded[22]); for Ge and As, 4s, 4p, and 4d (4d downfolded). To model the structure of Re_3GeAs_6, we chose complete Ge/As ordering on the 16f site (E2), realized in the space group $R\bar{3}m$. The integrations in k space were performed by an improved tetrahedron method[23] on 417 independent k points of a grid of 4096 k points evenly spread throughout the first Brillouin zone.

Physical Property Measurements. To investigate the high-temperature stability of Re_3GeAs_6, we performed a combined differential scanning calorimetry (DSC) and thermogravimetry (TG) measurement with the computer controlled NETZSCH STA 409PC Luxx between room temperature and 1120 K with a heating rate of 20 K/min. The measurement was carried out under a constant flow of argon (50 mL/min) to protect the thermocouples from potential As vapor, and a second stream of argon (flow of 30 mL/min) was directed over the balance.

For transport measurements, the samples of Re_3GeAs_6, $Re_3Ge_{0.8}As_{6.2}$, $Re_3Ge_{0.6}As_{6.4}$, and $Re_3Ge_{0.4}As_{6.6}$ were thoroughly ground. Parts thereof were then pressed into pellets of the dimensions 6 × 1 × 1 mm. The densities achieved via this pressing method were 9.0(2) g cm^{-3}, i.e., 83% of the ideal density as determined via neutron diffraction. These pellets were used to measure Seebeck coefficient, S, and electrical conductivity, σ, at Waterloo. A commercial thermopower measurement apparatus (MMR Technologies) was used to measure S under a dynamic vacuum, using constantan as an internal standard to determine the temperature difference. Silver paint (TED PELLA) was used to create the electric contacts. σ was determined via a four-point method: a custom-made device was used to determine the voltage drops ΔV over distances (L) of approximately 2 mm. The resistance, R, was calculated from the voltage drops using Ohm's law, i.e., $R = \Delta V/I$, with I = current. σ was calculated after measuring the

(19) Yin, S.-C.; Rho, Y.-H.; Swainson, I.; Nazar, L. F. *Chem. Mater.* **2006**, *18*, 1901−1910.
(20) Larson, A. C.; von Dreele, R. B. *GSAS−General Structure Analysis System*; Los Alamos National Laboratory: Los Alamos, NM, 2000.
(21) Hedin, L.; Lundqvist, B. I. *J. Phys. C* **1971**, *4*, 2064−2083.
(22) Lambrecht, W. R. L.; Andersen, O. K. *Phys. Rev. B* **1986**, *34*, 2439−2449.
(23) Blöchl, P. E.; Jepsen, O.; Andersen, O. K. *Phys. Rev. B* **1994**, *49*, 16223−16233.

Table 3. Seebeck Coefficient and Electrical Conductivity at 300 K of Cold-Pressed Pellets; Values for Hot-Pressed Pellets of the Same Samples are Given in Parentheses

	Re_3GeAs_6	$Re_3Ge_{0.8}As_{6.2}$	$Re_3Ge_{0.6}As_{6.4}$	$Re_3Ge_{0.4}As_{6.6}$
S (μV K^{-1})	−84 (−67)	−87	−88 (−72)	−87
σ (Ω^{-1} cm^{-1})	6 (760)	42	60 (1090)	47

lengths between the contacts, L, according to $\sigma = L/(AR)$, with the area $A = 1$ mm $\times$ 1 mm.

The results of these measurements at 300 K are summarized in Table 3. Evidently the Seebeck coefficient does not vary much within this series, and $Re_3Ge_{0.6}As_{6.4}$ exhibits the largest electrical conductivity. Subsequently, this sample and the electron-precise material Re_3GeAs_6 were shipped to Clemson for a complete determination of the physical properties.

At Clemson, both samples were again thoroughly ground and then pressed into round pellets with a diameter of 12.7 mm. The pellets were hot-pressed and densified at 1000 K under a weight of 2.3 tons for 90 min in an argon atmosphere (Thermal Technology HP20-4560-20). This procedure resulted in densities close to 91% of the ideal density. Seebeck coefficient and electrical conductivity were measured concurrently over a temperature range of about 9−328 K using a custom designed apparatus.[24] High-temperature Seebeck coefficient and electrical conductivity data were simultaneously determined up to 1000 K in a similarly customized apparatus equipped with a resistance furnace. Thermal conductivity was measured using the steady-state technique from 20 to 310 K using a custom-designed sample puck that plugs into the cold finger of a closed-cycle refrigerator.[25] All these measurements were performed under a vacuum as well. For more details, the reader is referred to a recent review article.[26]

High-temperature thermal conductivity data were determined from thermal diffusivity and specific heat measurements. Thermal diffusivity, α, was measured by a standard laser flash system (NETZSCH LFA 457). Specific heat, C_P, was measured with the NETZSCH DSC system using the differential scanning calorimetry (DSC) technique in which the heat flow rate to the sample is monitored. Then the thermal conductivity is calculated via $\kappa = \rho\alpha C_p$, with ρ = density.

Results and Discussion

Crystal Structures. Common features of the antimonides of the skutterudite family as well as of Mo_3Sb_7 are a complex cubic body-centered cell, squares of Sb atoms, and holes that may be filled with small cations.[27] Re_3GeAs_6 is a ternary substitution variant, where the squares between the cations are formed by As atoms (As1), and cubes are formed by Ge and As atoms (E2). The chains of Re_3GeAs_6 are comprised of the sequence E2 cube−Re−As1 square−Re−E2 cube−Re− ... Three such chains penetrate each other at the E2 cube (Figure 1).

Parallel running chains are interconnected via short E2−E2 bonds of 2.53 Å. These bonds, the shortest of this structure (Table 4), are slightly longer than single bonds, noting that Ge and As have comparable sizes. For example, the Pauling single bond radii[28] are 1.24 Å for Ge and 1.21 Å for As. This bond is concluded to be the main reason for the Ge atoms to prefer this site, as there are no homonuclear contacts between the As1 atoms <3.0 Å. Typically, for compounds with two anionic constituents of neighboring groups, the atom with the smaller electronegativity, in general the atom with the smaller group number, prefers the site with more and shorter anion−anion contacts, as may be seen in the NbPS type with its many examples,[29−31] and similarly in the Zintl phases Na_4KGeAs_3[32] and Cs_5GeAs_3.[33]

Correspondingly, the longer interactions between the main group elements of 2.90 and 3.09 Å are expected to be significantly weaker. As well, the bond between the transition metal atoms (here, Re−Re = 2.77 Å) is significant, although longer than a single bond (Pauling single bond radius of Re:= 1.28 Å). The same observations were made in the cases of $Mo_3Sb_5Te_2$ and $Nb_3Sb_2Te_5$.

The unit cell of Re_3GeAs_6 is slightly larger (0.2%) than that of Re_3As_7, with $a = 8.73180(7)$ Å vs 8.7162(7) Å, with $Re_3Ge_{0.6}As_{6.4}$ being intermediate ($a = 8.7287(3)$ Å), likely related to a Ge atom being slightly larger than an As atom. Because the atomic positions remain unchanged within their standard deviations, the structural changes are minimal. In either case, filling the E2 cube with a rattler atom may be of interest in attempts to lower the thermal conductivity.[27] Because the distance of the center to the corners occupied by either Ge or As atoms amounts to 2.52 Å, a number of cations (Mg, Fe, Co, Ni, ...) might fit into the cube. Such possibilities will be explored in the near future. Because the addition of a cation would enlarge the number of valence electrons, it would not help to render Re_3As_7 semiconducting, which already exhibits too many valence electrons for semiconductivity. Therefore, the incorporation of Ge (or possibly Si, Sn) remains necessary to achieve semiconducting properties when adding additional cations.

Electronic Structure. As revealed in Figure 2, the density of states (DOS) of the models chosen for $Mo_3Sb_5Te_2$ and Re_3GeAs_6 exhibit comparable features advantageous for thermoelectrics. First, this includes a band gap at the Fermi level, one of the major criteria for thermoelectrics. The larger (computed) gap of Re_3GeAs_6 of 0.9 eV ($Mo_3Sb_5Te_2$: 0.45 eV) implies that intrinsic Re_3GeAs_6 should exhibit a larger Seebeck coefficient and a smaller electrical conductivity, compared to $Mo_3Sb_5Te_2$. Moreover, it should reach its maximal ZT value at higher temperatures, for the band gap is proportional to the optimal temperature.[34] However, as the actual ordering of the Ge atoms is not known, the calculation based on the model in $R\bar{3}m$ can only be a crude approximation.

(24) Pope, A. L.; Littleton, R. T., IV; Tritt, T. M. *Rev. Sci. Instrum.* **2001**, *72*, 3129−3131.
(25) Pope, A. L.; Zawilski, B.; Tritt, T. M. *Cryogenics* **2001**, *41*, 725−731.
(26) Tritt, T. M. In *CRC Handbook on Thermoelectrics*; Rowe, D. M., Ed.; CRC Press: Boca Raton, FL, 2005.
(27) Soheilnia, N.; Dashjav, E.; Kleinke, H. *Can. J. Chem.* **2003**, *81*, 1157−1163.
(28) Pauling, L. *The Nature of the Chemical Bond*, 3rd ed.; Cornell University Press: Ithaca, NY, 1948.
(29) Donohue, P. C.; Bierstedt, P. E. *Inorg. Chem.* **1969**, *8*, 2690−2694.
(30) Huang, F. Q.; Flaschenriem, C.; Brazis, P.; Kannewurf, C. R.; Ibers, J. A. *Inorg. Chem.* **2003**, *42*, 3194−3198.
(31) Soheilnia, N.; Kleinke, K. M.; Kleinke, H. *Chem. Mater.* **2007**, *19*, 1482−1488.
(32) Eisenmann, B.; Klein, J. *Z. Kristallogr.* **1991**, *197*, 279−280.
(33) Eisenmann, B.; Klein, J.; Somer, M. *Angew. Chem., Int. Ed.* **1990**, *29*, 87−88.
(34) Sofo, J. O.; Mahan, G. D. *Phys. Rev. B* **1994**, *49*, 4565−4570.

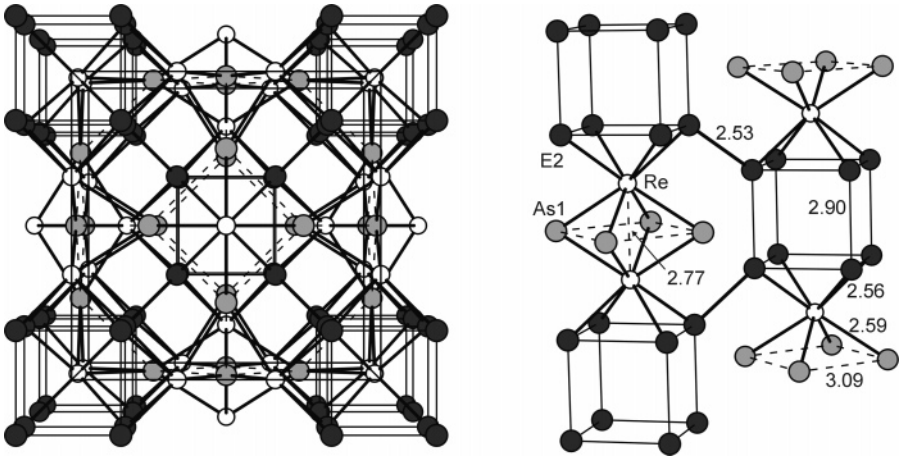

Figure 1. Structure (left) and two parallel running chains (right) of Re_3GeAs_6. White circles, Re; gray, As1; black, E2 (25% Ge2, 75% As2). Distances are given in angstroms.

Table 4. Selected Interatomic Distances (Å) of Re_3GeAs_6; E2: 25% Ge, 75% As

interaction	mult.	distance (Å)
Re−As1	4×	2.586(1)
Re−E2	4×	2.560(2)
Re−Re	1×	2.772(4)
As1−As1	2×	3.08716(3)
E2−E2	1×	2.533(5)
E2−E2	3×	2.904(3)

Second, the DOS both exhibit considerably drastic increases (spikes) directly above the gap and below the gap. This should lead to a large Seebeck coefficient, S, for both *n*- and *p*-type doped materials, which is proportional to the first derivative of the DOS. This may be deduced from the Mott eq 2, with the electrical conductivity being proportional to the DOS, with k_B = Boltzmann constant, T = temperature, e = charge of an electron, E = energy, E_F = Fermi energy, σ = electrical conductivity.[35,36]

$$S = \frac{\pi^2 k_B^2}{3e} T \left| \frac{\partial[\ln \sigma(E)]}{\partial E} \right|_{E = E_F} \quad (2)$$

Physical Properties. Both Re_3GeAs_6 and $Re_3Ge_{0.6}As_{6.4}$ are *n*-type materials, in contrast to the *p*-type thermoelectric $Mo_3Sb_{5.4}Te_{1.6}$. The Seebeck coefficient of Re_3GeAs_6 and $Re_3Ge_{0.6}As_{6.4}$ increases smoothly with increasing temperature, reaching $-67\ \mu V\ K^{-1}$ and $-72\ \mu V\ K^{-1}$, respectively, at 300 K (Figure 3). For comparison, Gascoin et al. determined $+55\ \mu V\ K^{-1}$ at 300 K for $Mo_3Sb_{5.4}Te_{1.6}$ in the Jet Propulsion Laboratories (JPL),[12] whereas we measured $+49\ \mu VK^{-1}$. It is noted that we applied higher pressures and temperatures to prepare the pellet for the measurements, which may be the cause for the slight difference in the thermoelectric properties. Interestingly, the ZT values are then equivalent, as the smaller Seebeck coefficient occurs with larger electrical conductivity.[13]

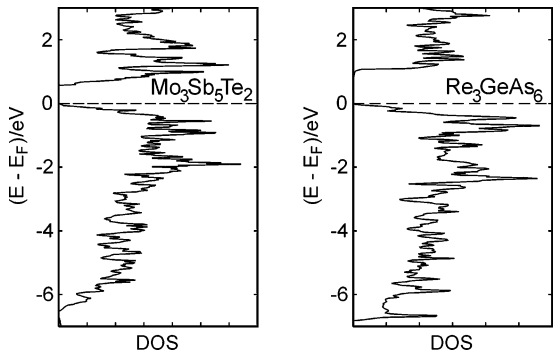

Figure 2. Density of states of $Mo_3Sb_5Te_2$ (left) and Re_3GeAs_6 (right). Dashed horizontal lines denote the Fermi level, E_F.

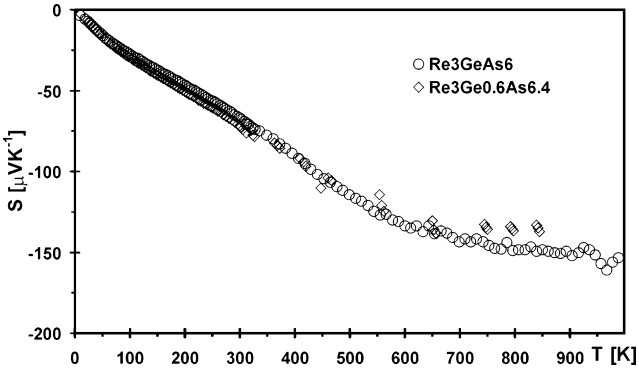

Figure 3. Seebeck coefficient of Re_3GeAs_6 (○) and $Re_3Ge_{0.6}As_{6.4}$ (◇).

The increase in S for the Re samples continues with the same slope up to 550 K, and thereafter the slope decreases, finally reaching around $-150\ \mu V\ K^{-1}$ at 900 K. The larger Seebeck coefficient of the Re samples correlates nicely with the larger band gap and the steeper slope of the DOS. For $Re_3Ge_{0.6}As_{6.4}$ and $Mo_3Sb_{5.4}Te_{1.6}$, the observation of *n*- and *p*-type follows directly from electron counting, as the former exhibits more than 55 valence electrons per formula unit, namely 55.4, and the latter less (54.6).

As expected on the basis of the density of states, $Re_3Ge_{0.6}As_{6.4}$ and Re_3GeAs_6 have significantly smaller electrical conductivity ($1090\ \Omega^{-1}\ cm^{-1}$ and $760\ \Omega^{-1}\ cm^{-1}$ at 300 K) than $Mo_3Sb_{5.4}Te_{1.6}$, determined to be $1610\ \Omega^{-1}\ cm^{-1}$ by Gascoin et al. and $1780\ \Omega^{-1}\ cm^{-1}$ by us. In either case, the electrical conductivity decreases slowly with increasing temperature (Figure 4), typical for degenerate semiconductors. The observation that the electron-precise material Re_3GeAs_6 exhibits such high electrical conductivity is indicative of a high concentration of defects and/or disorder.

(35) Mott, N. F.; Jones, H. *The Theory of the Properties of Metals and Alloys*; Dover Publications: New York, NY, 1958.
(36) Mahan, G. D.; Sofo, J. O. *Proc. Natl. Acad. Sci. U.S.A.* **1996**, *93*, 7436−7439.

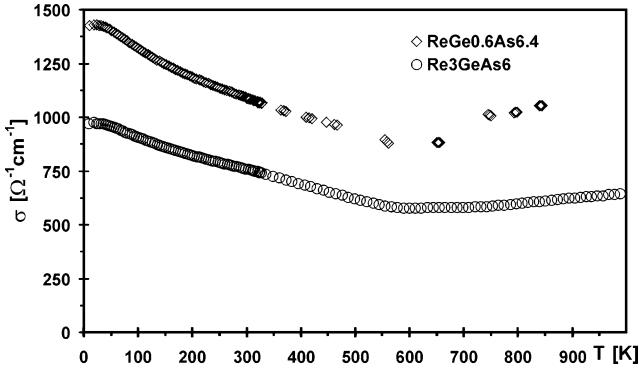

Figure 4. Electrical conductivity of Re_3GeAs_6 (○) and $Re_3Ge_{0.6}As_{6.4}$ (◇).

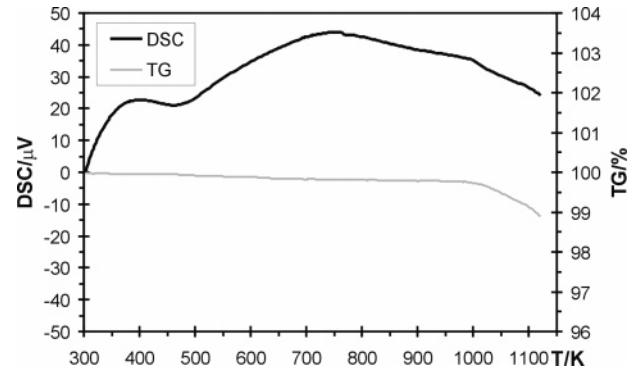

Figure 5. Thermal analysis of Re_3GeAs_6.

As is the case for the Seebeck coefficient, the slope of the electrical conductivity changes around 550 K, where the conductivity commences to increase. On the other hand, the DSC measurement shows no peak around 550 K (Figure 5); we note that the shape of the DSC curve is determined by the device,[37] i.e., no phase transition was detected. Weight loss becomes significant around 1000 K.

A comparison of the power factor P.F. $= S^2\sigma$, the numerator of ZT that determines the electrical performance of a thermoelectric, is instructive. At 300 K, we calculate P.F. to be 4.3 μW cm^{-1} K^{-2} for $Mo_3Sb_{5.4}Te_{1.6}$, 5.7 μW cm^{-1} K^{-2} for $Re_3Ge_{0.6}As_{6.4}$, and 3.4 μW cm^{-1} K^{-2} for Re_3GeAs_6. The changes in the trends of the Seebeck coefficient and the electrical conductivity are reflected in a decrease of the slope of the power factor of Re_3GeAs_6, becoming apparent above 600 K. On the other hand, the power factor of $Mo_3Sb_{5.4}Te_{1.6}$ continues its linear increase up to 1000 K, as published by Gascoin et al. (Figure 6).[12] Nevertheless, the power factor of $Re_3Ge_{0.6}As_{6.4}$ remains larger than that of $Mo_3Sb_{5.4}Te_{1.6}$ throughout the whole temperature range measured, reaching 19 μW cm^{-1} K^{-2} at 840 K, compared to 15 μW cm^{-1} K^{-2} of $Mo_3Sb_{5.4}Te_{1.6}$, whereas the power factor of Re_3GeAs_6 begins to fall below that of $Mo_3Sb_{5.4}Te_{1.6}$ around 600 K, for example, with P.F.(840 K) = 13.5 μW cm^{-1} K^{-2}.

Last, the thermal conductivity, κ, increases from 20 to about 100 K, and then more or less reaches a plateau between 300 and 400 K before starting to decrease (Figure 7). The room-temperature values are 4.2 W m^{-1} K^{-1} for $Re_3Ge_{0.6}As_{6.4}$ and 3.9 W m^{-1} K^{-1} for Re_3GeAs_6. We observed a similar temperature dependence for $Mo_3Sb_{5.4}Te_{1.6}$,

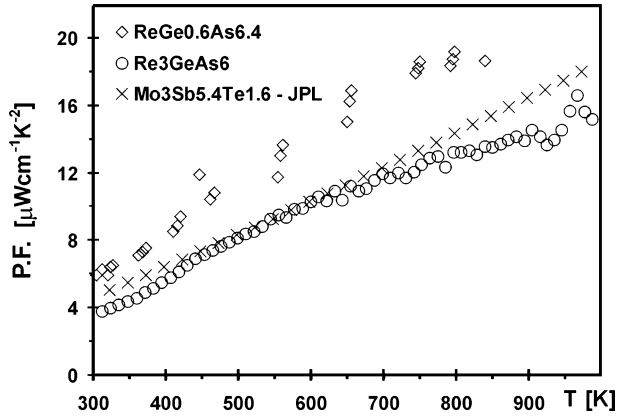

Figure 6. Power factors of Re_3GeAs_6 (○) and $Re_3Ge_{0.6}As_{6.4}$ (◇), compared to JPL's data on $Mo_3Sb_{5.4}Te_{1.6}$ (×).

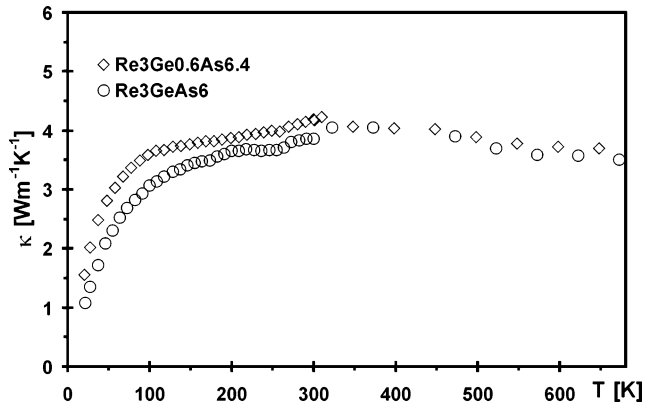

Figure 7. Thermal conductivity of Re_3GeAs_6 (○) and $Re_3Ge_{0.6}As_{6.4}$ (◇).

with κ(300 K) = 4.4 W m^{-1} K^{-1}, which compares nicely to the numbers from Gascoin et al.

The thermal conductivity is comprised of the lattice thermal conductivity, κ_L, and the electronic thermal conductivity, κ_E: $\kappa = \kappa_L + \kappa_E$. Via the Wiedemann−Franz relationship, one can calculate κ_E when the electrical conductivity, σ, is known (with L_0 = Lorentzian number)[38]

$$\kappa_E = L_0 \sigma T \tag{3}$$

Using eq 3, one obtains very comparable values of the lattice thermal conductivity at 300 K for all three cases, namely 3.3 W m^{-1} K^{-1} for Re_3GeAs_6, 3.4 W m^{-1} K^{-1} for $Re_3Ge_{0.6}As_{6.4}$, and 3.5 W m^{-1} K^{-1} for $Mo_3Sb_{5.4}Te_{1.6}$. It is concluded that the differences in the thermal conductivity largely stem from the different electronic contributions, not surprisingly, as the structures, bonding, and molar masses of these materials are very similar.

From the results of our measurements shown in Figures 3, 4, and 7, the thermoelectric figure-of-merit, ZT, was calculated via eq 1. ZT increases rapidly with increasing temperature in all three cases (Figure 8), and $Mo_3Sb_{5.4}Te_{1.6}$ and Re_3GeAs_6 exhibit almost identical slopes as well as values. Most intriguingly, the ZT values of $Re_3Ge_{0.6}As_{6.4}$ are significantly larger than those determined for $Mo_3Sb_{5.4}Te_{1.6}$, e.g. ZT(300 K) = 0.041 vs 0.029 and ZT(700 K) = 0.30 vs 0.27, and follow a comparable slope as far as measured, i.e.,

(37) Soheilnia, N.; Dashjav, K. M. K.; Cuthbert, H. L.; Greedan, J. E.; Kleinke, H. *Inorg. Chem.* **2004**, *43*, 6473−6478.

(38) Kittel, C. *Introduction to Solid State Physics*, 7th ed.; John Wiley & Sons, Inc.: New York, 1996.

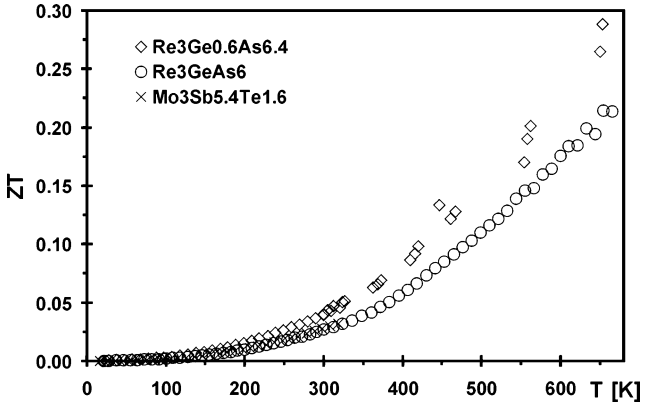

Figure 8. Thermoelectric figure of merit of Re_3GeAs_6 (○) and $Re_3Ge_{0.6}As_{6.4}$ (◇), compared to $Mo_3Sb_{5.4}Te_{1.6}$ (×), which overlaps with the Re_3GeAs_6 values.

until 700 K. Moreover, because the lattice thermal conductivity of all these materials is basically equivalent, and the electrical contribution is lower in case of the Re samples, as deducted from the electrical conductivity measurements via eq 3, one can assume lower total thermal conductivity at higher temperatures as well. This combined with the higher power factor of $Re_3Ge_{0.6}As_6$ at least up to 840 K leads to the extrapolation of a significantly higher ZT value, compared to $Mo_3Sb_{5.4}Te_{1.6}$.

Conclusion

Chemical modification of the metallic arsenide Re_3As_7 by partial Ge substitution for As led to the formation of new thermoelectric materials, Re_3GeAs_6 and $Re_3Ge_{0.6}As_{6.4}$. These materials are isostructural with $Mo_3Sb_{5.4}Te_{1.6}$ (Ir_3Ge_7 type), one of the leading high-temperature *p*-type thermoelectrics. The Re compounds exhibit higher Seebeck coefficient and lower electrical conductivity compared to $Mo_3Sb_{5.4}Te_{1.6}$, as expected on the basis of our electronic structure calculations. The lattice thermal conductivity of these three compounds is almost identical. $Re_3Ge_{0.6}As_{6.4}$ is an *n*-type semiconductor with larger thermoelectric figure of merit, ZT, than $Mo_3Sb_{5.4}Te_{1.6}$ at least up to 700 K. In contrast to $Mo_3Sb_{5.4}Te_{1.6}$, the temperature dependencies of the thermoelectric properties of Re_3GeAs_6 do not continue smoothly beyond 550 K, whereas the power factor of $Re_3Ge_{0.6}As_{6.4}$ is the largest of this series up to 840 K. Why the trends of the physical properties change around 550 K needs to be investigated. Further research will reveal how far these materials can be further improved by intercalation of small cations, as well as partial Sn/As exchange.

Acknowledgment. Financial support from NSERC, CFI, OIT (Ontario Distinguished Researcher Award for H.K.), MMO, and the Canada Research Chair program (CRC for H.K.) is appreciated. Support from a DOE/EPSCoR Implementation Grant (DE-FG02-04ER-46139) is acknowledged, as is support from the SC EPSCoR Office/Clemson University cost sharing for the work highlighted in this publication.

Supporting Information Available: Two plots depicting the Rietveld refinements on Re_3GeAs_6 and $Re_3Ge_{0.6}As_{6.4}$, and one table showing crystallographic details of the latter (PDF). This material is available free of charge via the Internet at http://pubs.acs.org.

CM0708517